Structural Model for Dry-Drawing of Sheets and Yarns from Carbon Nanotube Forests

Alexander A. Kuznetsov,[†] Alexandre F. Fonseca,[†,‡] Ray H. Baughman,[†] and Anvar A. Zakhidov[†,*]

[†]Alan G. MacDiarmid NanoTech Institute, University of Texas at Dallas, Richardson, Texas 75083, United States and [‡]Departamento de Física, Instituto de Ciencias Exatas, Universidade Federal Fluminense, Volta Redonda, RJ, 27213-415, Brazil

ABSTRACT A structural model is developed for describing the solid-state transformation of a vertically oriented carbon multiwall nanotube (MWNT) forest to a horizontally oriented MWNT sheet or yarn. The key element of our model is a network of individual carbon nanotubes or small bundles interconnecting the array of main large-diameter MWNT bundles of the forest. The dry-draw self-assembly mechanism for MWNT sheet formation involves two principal processes that reconfigure the interconnection network: (1) unzipping by preferentially peeling off interconnections between the bundles in the forest and (2) self-strengthening of these interconnections by densification at the top and bottom of the forest during draw-induced reorientation of the bundles. It is shown that interconnection density is a key parameter that determines the ability of a MWNT forest to be dry-drawable into sheets and yarns. This model describes the principal mechanism of solid-state draw (confirmed by dynamic *in situ* scanning electron microscopy), the range of forest structural parameters that enable sheet draw, and observed dependencies of sheet properties on the parent MWNT forest structure.

KEYWORDS: carbon nanotubes · sheets · yarns · dry-spinning · dry-drawing

Following the pioneering work of Jiang *et al.*[1] on the solid-state fabrication of carbon nanotube (CNT) yarn by nanotube draw from a CNT forest, we demonstrated that the strength of these yarns could be increased a thousand-fold by inserting twist during spinning.[2] Also, we found that indefinitely wide CNT sheets can be drawn from forests having suitable structure.[3] Other groups have also reported the ability to draw long CNT yarns directly from CNT forests[4−11] and have provided important additional information. Interest in these solid-state processed CNT sheets and yarns is great because of potential applications for electronic textiles, supercapacitors, flexible transparent conductive electrodes (for solar cells, OLEDs, generic displays, and smart windows), light sources, optical polarizers, and artificial muscles, among others.[2,3,7,12,13]

Although CNT forests can be produced over a broad range of conditions, very special conditions are required to grow CNT forests suitable for solid-state fabrication of sheets and yarns. We call these special CNT forests simply *drawable* CNT forests. Though drawability depends upon good alignment of CNT bundles,[4,14] we find that it also and most importantly depends on the type of structural interconnections between CNTs within the forest. In order to understand the conditions for drawability, we analyzed the transformations during the draw process by using dynamic *in situ* SEM imaging and performing experiments on tensile forces during draw. On the basis of this analysis we have developed a model explaining the relationships between sheet drawability, forest structure, and the structural transformations during sheet draw.

Sequential SEM micrographs showing the draw of a MWNT sheet from a MWNT forest (see Figure S1 and Movie S1 in the Supporting Information) show the 90° reorientation of vertically aligned bundles in the forest to horizontal alignment in the sheet. In this case the forest comprised 300 μm long nanotubes with 10−15 nm diameter that are largely present as ~50 nm diameter bundles.

This process suggests the existence of relatively strong adjacent forces between the bundles of CNTs in the forests that could, *a priori*, be explained only by van der Waals interactions. Since the more uniform the contact areas among two systems, the stronger the van der Waals forces between them, a good vertical alignment of the CNTs seems to explain the origin of the drawability of the forest. However, a more careful analysis of the pulling out process shows that alignment and van der Waals forces alone are not enough to describe the full conditions for *drawability*. If the external pulling out forces are strong enough to bend the first bundle and peel it off from the vertical next bundle, then how can van der Waals forces alone explain that just

*Address correspondence to zakhidov@utdallas.edu.

Received for review September 14, 2010 and accepted January 14, 2011.

Published online February 04, 2011
10.1021/nn102405u

before the full detachment of the first bundle, the next bundle starts being pulled out? Why do the strong external forces not simply detach the first bundle completely from the forest, thus terminating continuous draw? Do, for some reason, the van der Waals forces get stronger at the extremities of the bundles, *i.e.*, at the top and bottom of the forest? Or is there some other mechanism behind this process? Zhang *et al.*'s model[4] cannot answer these questions. We first thought[2,3] that some kind of entanglement at the extremities of the bundles should be the origin responsible for the connection between the adjacent bundles at their ends. Zhang *et al.*[8] also suggested that the entanglement at the extremities of the forests should be the mechanism behind the connection between the bundles of nanotubes. But the analysis of nondrawable forests shows that their level of entanglement is even higher than that for the drawable forests, suggesting that the entanglement at the ends is not the main factor. We can see from Movie S1 (Supporting Information.) that the upper extremity, *i.e.*, top part of the CNT forest, does not present higher entanglement.

Another question comes from the analysis of the structure of the as-produced sheets and yarns. Their large longitudinal stiffness shows that the longitudinal connections between the bundles should be somehow stronger than simply given by the model in ref 4.

In order to explain the pulling-out process and answer the above questions consistently, we build a model for the structure of a drawable CNT forest based not only on vertically aligned bundles but mostly on the existence of a network of special interconnections between bundles. The model introduces two novel concepts: the "unzipping of interconnections" phenomenon generated by a peeling-off/stick process between interbundle connections and main bundles during rotational movement of bundles from the vertically oriented forests of CNTs to horizontal CNT sheet; the self-strengthening of the interbundle nanotube interconnections at the top and bottom of the forest as a consequence of the multiple unzipping processes leading to densification. We emphasize that in our model van der Waals forces between vertical big bundles and interconnecting nanotubes play a major role in the process of unzipping the interconnections. The van der Waals forces between neighboring vertical big bundles are much weaker due to larger separation distance.

These two concepts will be explained in the next sections. Experimental evidence will be presented to support our model. To the best of our knowledge, there is no other model for the dry-drawing process that properly explains the existence of the window of forest heights and densities in which the dry-drawing is possible.

RESULTS AND DISCUSSION

Description of the Model for Solid-State Draw. Scanning electron micrographs (as well as Movie S1) show that conversion of nanotube forests to nanotube sheets is a complex many-body problem. However, by tracking individual bundles in the Movie S1 (taken parallel to a forest edge and orthogonal to both the sheet thickness and width direction) we can understand a fundamentally important process: drawing a first forest tree from a forest starts with bending this forest tree from its initial vertical orientation, while forest connects are being unzipped from or onto neighboring trees (which initially remain in the forest). Together with results presented herein, the bending process can also be clearly seen in Figure 12 of ref 9.

Let us refer to the CNT direction in the forest as the "z" axis, the draw direction as the "x" axis, and "y" as the axis perpendicular to both "x" and "z". Just before being completely detached from the forest, the first bundle starts pulling out the next vertical bundle (in the same $z-x$ plane), and the process now goes in the opposite direction; that is, if the first bundle (forest tree) is peeled off (unzipped) from the forest bottom, the next forest tree will be pulled off from the top. This process continuously repeats for successive forest trees.

On the basis of this observation, we conclude that the original forest consists of vertically oriented forest trees (big bundles) with an average diameter of 50−100 nm interconnected by smaller bundles or individual nanotubes (connects) with an average diameter of 10−20 nm. A two-dimensional schematic illustration of the as-grown array of forest trees (big bundles) and connects (smaller bundles or individual nanotubes) is shown in Figure 1, left. The color of the connect is the same as for the forest tree from which it will be unzipped during the draw.

In order to understand the role of connects in the drawing process, first consider two forest trees that are bridged by a single connect. The corresponding process of reorienting vertical forest trees into horizontal position is illustrated in Figure 1, right. The connect shown in Figure 1, right, is detached from the left forest tree during the draw of the right forest tree and is attached to the right one by van der Waals forces. We call this process of partially detaching a connect from one forest tree and adhering it on the neighboring forest tree (using van der Waals forces) the "*unzipping*". The net result of this process is that connects alternatively concentrate during draw at either the top or bottom of forest trees, both during the draw process and in the final sheet or yarn. In Section 3 we explain this mechanism and the relation between the magnitudes of the forces F_1 and F_2 shown in the detail of Figure 1, right.

In the presence of more interconnections between forest trees, all of them will "unzip" in the same way and get concentrated in their bottom or top part as long as more interconnections continue to unzip. Eventually their number will reach some critical value, and these interconnections will have enough force to start pulling

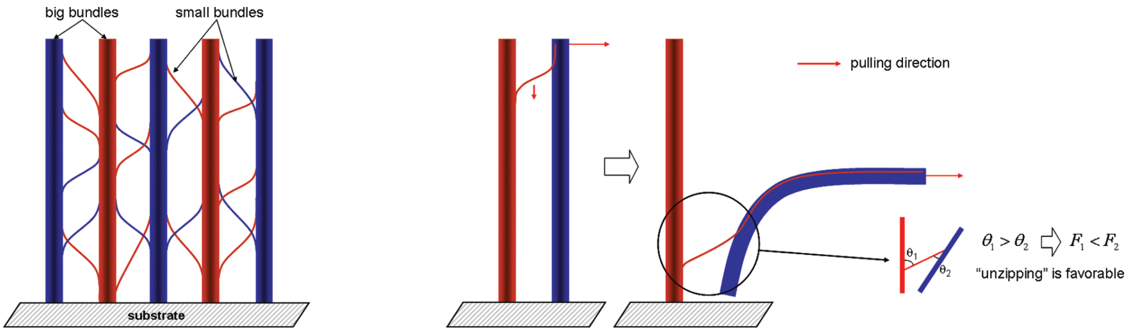

Figure 1. Left: Schematic picture of a nanotube forest consisting of vertically oriented big bundles (forest trees) and interconnecting small bundles or individual nanotubes (connects). Right: The *unzipping*−*zipping process* results in movement of the connects along the forest tree lengths, so as to concentrate these connects at forest tree ends. In the detail, the angles of peeling at both adjacent bundles and the respective forces F_1 and F_2 are indicated. Red arrow represents the external force used for the draw.

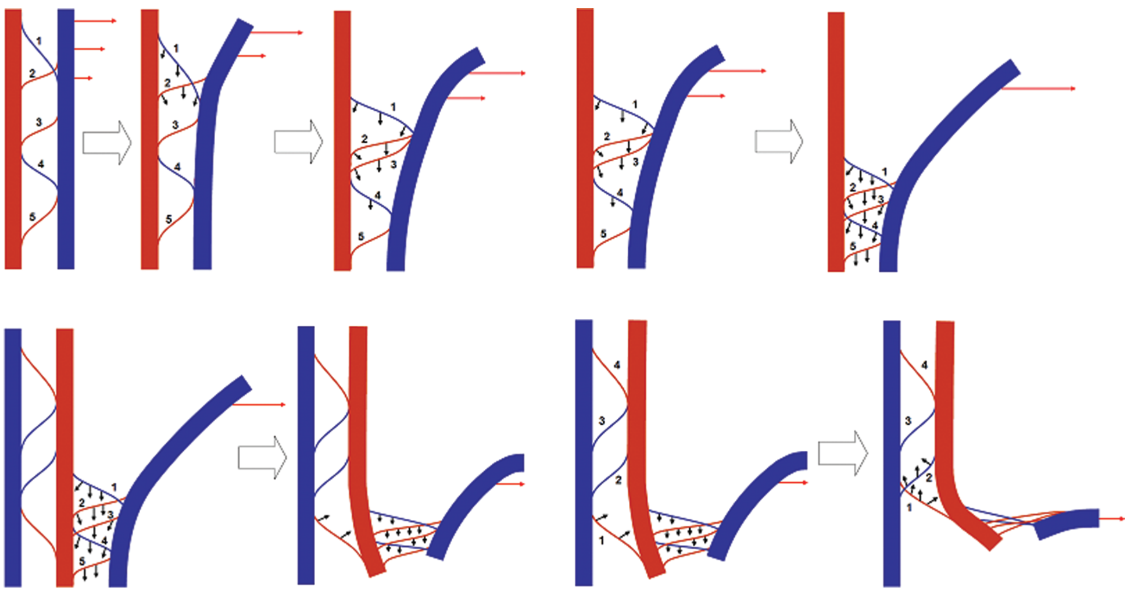

Figure 2. Scheme of the process of *pulling out* a forest tree from the forest. Blue and red bars represent forest trees or bundles of CNTs, and the separation distance between them is increased for clarity. Red arrows show the external force applied to the first bundle. Small black arrows show the direction of the net movement of the interconnections.

out the next forest tree (Figure 2). Figure S2 shows SEM images of the typical moment when a forest tree starts to pull the next one out of the forest.

The key parameter of the model is, then, the number of interconnections between the forest trees. The process described above qualitatively sets the top and bottom limit to the interconnection density parameter, and hence the limiting minimal and maximal heights of CNT forests. If the interconnection density is small, *i.e.,* forest is low (Figure 3A), then the external pulling force divided by the number of interconnections will be large enough to peel each interconnection completely off the next forest tree, thus interrupting the pulling process. Experimentally it is observed when the CNT forest is not high enough (typically below 50−80 μm).

On the other side, if the interconnection density is large (Figure 3B), the next forest tree will be pulled out from somewhere before the middle. In this case, the pulling process will also be terminated. Since the CNT bundles that form the forest trees are very stiff with respect to stretching, the second forest tree cannot be continuously bent in the *x* direction starting from its middle (as Figure 3B illustrates) and keep its vertical parts at the same distance from the third forest tree without conserving its total length. So one of the following will happen: (1) the second forest tree completely detaches from the forest; or (2) the interconnections between the second and third forest tree are strong enough to pull out the third forest tree as a whole; then forest trees do not form the fiber and eventually get ruptured. Experimentally, if the forest is too high (typically higher than 800 μm), big "chunks" of nanotubes get separated from it and make drawing impossible.

Since the interconnections between the CNT bundles are not only in the *z*−*x* plane, we extend the described process to a three-dimensional case (Figure S3).

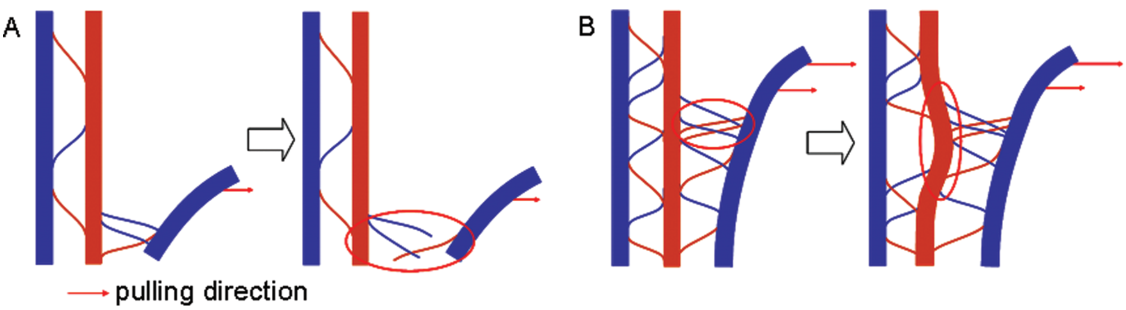

Figure 3. Predicted effects of low (A) and high (B) interconnection density on the pulling-out process.

There are numerous 2-D processes going simultaneously in the $z-x$ plane, which are shifted by some phase delay because of the interconnections in the $z-y$ direction. The dependence of the phase delay on the geometric parameters of the CNT forest is briefly analyzed in the Supporting Information. This 3-D process of oriented horizontal CNT network formation and the 3-D structure of interconnections is extremely important for understanding the CNT optical polarizers' quality and the anisotropy of sheet resistance, as well as the electrostatic actuation. The overlapping of each peeling-off bundle can be seen in the Movie S1. Because of the interconnections in the $z-y$ plane, when pulling is started from only a single forest tree, it expands into a wide strip, as illustrated in Figure S3.

Estimate of the Minimum and Maximum Number of Interconnections. From the main features observed in the SEM images of the pulling-out process (Movie S1) we propose a model based on three properties of the CNT forests: (i) there should be individual nanotubes or small bundles laterally interconnecting the forest trees within the CNT forest; (ii) during the detachment of the first bundle, or forest tree, these interconnections should move in the same direction as the peeling off of this bundle, in a phenomenon we call the "*unzipping process*"; and (iii) the unzipping of a forest with many interconnections increases their density; at some point this concentration reaches its critical value and the external force starts pulling out the next bundle, as illustrated in Figure 2.

Properties i, ii, and iii are explained on the basis of the experimental and theoretical results obtained by us and other groups.

Property i: Existence of Lateral Interconnections. In order to support our deduced property number i, we present SEM images of the drawable CNT forests and the sheets pulled out from them. Figure 4 displays a drawable forest of MWNTs with a ~10 nm diameter, averaging 9 walls per tube. One can see many vertically oriented bundles of CNTs and lateral interconnections formed by individual nanotubes or small bundles. The number of interconnections is large, but not all of them contribute to the unzipping process. In the section highlighted by the red circle in Figure 4, the interconnection originates in the inferior part of the bundle and, after going to the right, goes back to the same original

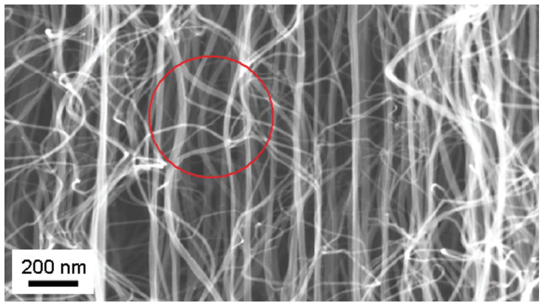

Figure 4. SEM image of the side view of a MWNT drawable CNT forest at high magnification. Inside the red circle, there is an example of an interconnection that does not contribute to the pulling-out process because it goes back to the bundle where it is originated from. See the text for details.

bundle. An interconnection like this does not contribute to the concentration of interconnections, because when the forest is pulled on the right it disconnects from the bundle. The observation of individual CNTs or small bundles interconnecting the main CNT bundles, within the CNT forest, was also reported by independent groups (Figure 1B of ref 4, Figure S6 of the Supporting Information of ref 14, and Figure 1b of ref 8).

Lateral interconnections confirm the proposed 3-D network of Figure S3. Since the interconnections along $z-y$ plane do not get concentrated as the longitudinal ones during the unzipping process, our model predicts that CNT sheets possess anisotropic mechanical properties. In the direction perpendicular to the pulling-out process of a CNT sheet, from now on called "*lateral direction*", the stiffness is much less than that along the pulled-out fibers. We have recently discovered a CNT sheet actuation phenomenon that experimentally confirms this anisotropy.[12]

Property ii: Unzipping Process. Property number ii that determines the direction of the unzipping process is based on theoretical considerations. To understand unzipping, we apply Kendall's model,[15] which describes the process of peeling a thin film off a solid substrate:

$$\frac{F}{b}(1-\cos\theta)-R=0 \qquad (1)$$

where b is the width of the film, R is the adhesion energy, and θ is the angle between the direction of the

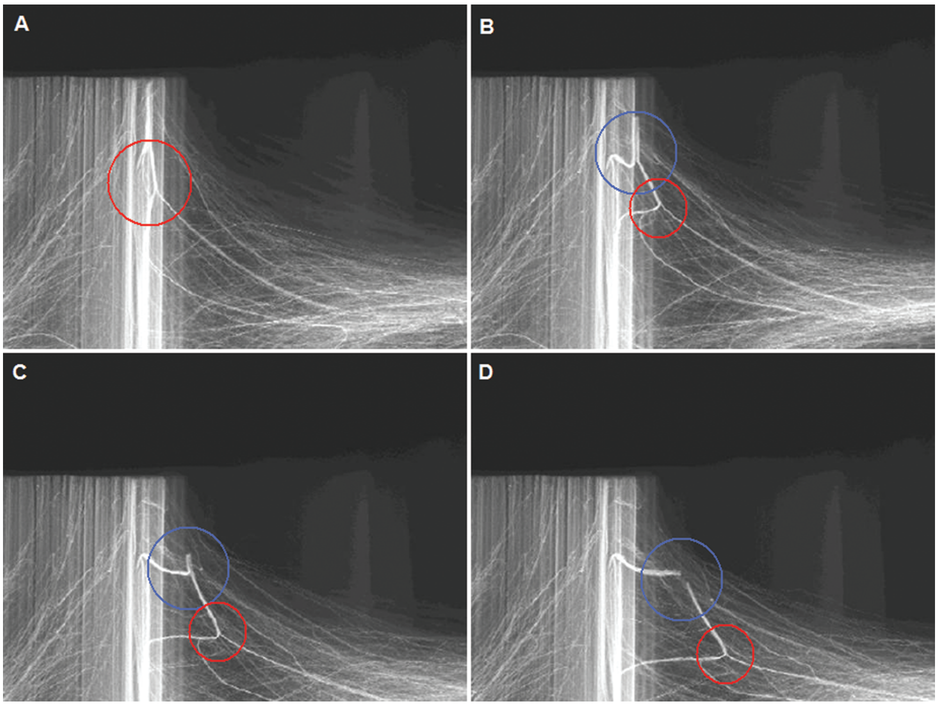

Figure 5. Sequence of consecutive SEM images, given by panels from A to D, of the side view of the CNT forest during the pulling-out process. Red circles show the sequences of points where a pulled-out bundle started pulling the next bundle. Blue circles show the rupture of two adjacent bundles. See the text for more details.

applied force F and the substrate. The scheme on the right of Figure 1 shows how these parameters determine the "unzipping" process in forest drawing. When pulling out a bundle from top to bottom, the force that attaches the interconnection to the right bundle (F_2) is larger than the force to the bundle on the left (F_1) (see right bottom corner of Figure 1, right), since the angle θ on the right is smaller than that on the left. It makes the unzipping possible.

The same conclusion can be obtained for the case where the interconnection originates from the left bundle and terminates on the right bundle (see Supporting Information). A more quantitative analysis of the attaching forces between an interconnection and the respective bundles can be made on the basis of analytic expressions for the attractive forces between CNTs,[16] obtained from the universal graphitic potential proposed by Girifalco *et al.*[17] Our calculations (see Supporting Information) show that the forces on the interconnection lead to the same above result for the unzipping process.

The experimental support for property number ii comes from the recent work of Strus *et al.*[18] They measured the forces needed to peel off a MWNT from a highly ordered pyrolytic graphite (HOPG) surface. They used the previously mentioned analytical expression for the force per unit length needed for a separation between CNTs[16] to obtain good agreement between theory and experiment. They showed that the peeling forces vary with the distance between the MWNT and the HOPG surface, having a maximum value of ~10 nN. This value can be used to estimate the minimum value for the number of interconnections needed to have a drawable CNT forest.

Property iii: Critical Number of Interconnections. The idea of a critical value for the density of interconnections comes from the fact that the peeling process can be terminated by the complete detachment of the first bundle from the forest after reaching its extremity. However, since it does not happen in drawable CNT forests, there must exist other causes that start the pulling out of the next adjacent bundle. On the basis of the above property i and the scheme depicted by Figure 2, we propose the existence of a critical number of interconnections that is capable of transferring the external forces to the next bundle. The sequence of SEM images in Figure 5 supports this conclusion. Following the two connected bundles inside the blue circle (panels B to D), we see an example of what is expected to happen when we do not have our proposed structure of interconnections between the forest trees or the critical number of interconnections is not reached: the bundles simply detach from each other because of the external pulling-out forces. Now, looking at the connection between the bundles inside the red circle (panels A to D), we clearly see that for these bundles the external forces do not rupture them. van der Waals forces between the forest trees or big bundles cannot be responsible for these processes. Our proposed model of interconnections that, by the unzipping process, get concentrated at the forest extremities gives a consistent explanation for both phenomena.

The separation of the two bundles shown inside the blue circles (from panels B to D) occurs because the number of interconnections between those two bundles is not enough to form a critical value of connections to keep them together. In the case of the observed pulling out of one forest tree from the previously detached bundle, shown inside the red circles (from panels A to D), the number of interconnections between the bundles not only reached the critical value necessary to transmit the external force to next bundle but also achieved that value in a region before the previous bundle reached the upper extremity of the forest. According to our model, the density of interconnections between these two bundles should be larger than that between the other bundles, so they get the critical number of interconnections before the extremity. Since in a real forest the number of interconnections is not expected to be perfectly uniform, this case may happen several times, suggesting that there is a range of the number of interconnections for which the CNT forest is drawable.

The influence of the number of interconnections on the drawability of a CNT forest can be verified from the analysis of the nondrawable CNT forests. We have experimentally found that low-height forests are not drawable. Our model explains this result by the fact that for short CNT forests the number of interconnections never reaches the critical value to start pulling out the next bundle. Therefore, they cannot form CNT fibers by a dry-drawing process.

There is also an upper limit on the height of the CNT forests above which they are not drawable anymore. This was observed by other independent groups. Li *et al.*,[5] for example, reported that they were not able to pull out yarns from CNT forests of heights out of the range of 0.5 to 1.5 mm. The reason is that in CNT forests of larger heights but the same densities of interconnections the critical number of interconnections can be reached before the first bundle is close to the forest extremities. Then it starts pulling out the next bundle from the middle or even earlier (see previous section and Figure 3B), thus inhibiting the pulling-out process.

All experimental groups[1−9] that were able to pull out yarns and sheets agreed that the CNT forest must be formed by vertically aligned CNTs. Our model also relies on this property since more aligned CNT forests have a specific type of interconnections between the bundles like those depicted in Figure 1. These interconnections start on one bundle and end on the adjacent one. Forests formed by less vertical or *wavy* CNT bundles contact neighbor bundles directly more frequently and, then, by van der Waals forces, form what we call *direct interconnections*. When an external force pulls out this type of wavy CNT forest, the excess in the number of direct interconnections causes the rupture of the pulling-out process, since the external force is uniformly distributed along the bundles. In vertically aligned CNTs the interconnections that contribute to the unzipping process predominate since they have much fewer direct connections. Thus, it is possible to pull out sheets or yarns from much taller forests, provided they are formed by much more vertically aligned CNTs. This explains the results of Liu *et al.*,[14] where CNT sheets were drawn from different drawable CNT forests of different heights, all of them having good vertical alignment. In terms of our model, all Liu *et al.*[14] CNT forests did not reach the superior limit of height from which their CNT forests become nondrawable.

Our model, therefore, predicts the existence of a qualitative relationship between the level of vertical orientation of the CNTs, the level of interconnectivity between them within the forest, and the forest height. It predicts the existence of a range of heights, $L_{min} < L < L_{max}$, for which the dry self-assembly is possible.

We have performed a simple experiment in order to measure the smallest external force that can start to pull out a CNT fiber from a drawable CNT forest. The force required to pull a 1 mm wide sheet out of the forest is about 350 μN. This gives the minimum force to start pulling out one bundle of ~100 nN. A force required to bend a 15 μm long bundle of 100 MWNTs with a 10 nm diameter each (using expressions for continuous rods[19,20]) is estimated at ~1 nN in the softest limit case and ~100 nN in the hardest limit case. The softest limit refers to the case when the CNTs forming a bundle are free to slip along each other; in the hardest limit case the CNTs form a coherent bundle-crystal structure.[19] While the hardest bending force is at least 100 times larger than the softest force required to bend the bundle, the upper limit exactly matches the amount needed to start the pulling out. Since the bending is necessary for the unzipping process, as explained in the previous subsection, the initial force that starts the pulling-out process is required to overcome the bending stiffness of the bundles.

If we consider the value of the force necessary for peeling off a MWNT from a HOPG surface, $f_1 \approx 10$ nN,[18] then the minimum value of the force needed for pulling out our CNT forest, 100 nN, is 10 times that force. This suggests that, at minimum, we should have about 10 interconnections concentrated at the end of a tree, having the transfer of the external force of 100 nN to the next bundle, starting pulling it out from the forest. This value should be taken as a lower limit for the total number of interconnections, because the minimum contact force between the interconnections and the CNT bundles may vary depending on their surface properties such as the presence of defects, amorphous carbon, or the fact that the surface of the bundle is not as flat as that of a HOPG. Since it is known from experiments that the attachment of the bundles to the substrate is very weak, these forces can be neglected.

We can also estimate the upper limit of the number of interconnections for the drawability of a CNT forest, if we consider that at the lower limit the next bundle is pulled from its bottom (or top). Assuming the interconnections are uniformly distributed along the vertical direction of the bundle, it will require twice the minimum number of interconnections to start the pulling out of the next bundle in the middle (see Figure 3B). The unzipping process will then be terminated, because the third bundle will be pulled from both sides simultaneously. So the number of interconnections ρ_I is proposed to be in the following range:

$$\frac{f}{f_1} < \rho_I < 2\frac{f}{f_1} \quad (2)$$

where f is the total force required to pull the next bundle and f_1 is the force required to completely peel off an interconnection from the bundle. Using the values from ref 18 and our measurement of the minimum force to start the pulling-out process, we obtain the following range:

$$10 < \rho_I < 20 \quad (3)$$

However, these values are given for an ideal case in which the adhesion forces between interconnections and bundles are roughly the same as the ones between a nanotube of 40 nm of diameter and a flat surface of HOPG. Since the bundles are not so straight and the contact area between interconnections and bundles is smaller than that for the nanotube and HOPG, the force of adhesion falls below 10 nN, and more than 10 interconnections are required for the low limit of interconnections density, and by eq 2, twice as much for the high limit of density. In reality there are many more interconnections, but not all of them contribute to the drawability (Figure 4). Some of them might break or have too many defects to participate in the process. Future theoretical and experimental work on the peeling-off forces can provide more precise values for the range of the number of interconnections between adjacent CNT bundles for which the CNT forest is drawable.

Equation 2 allows to estimate minimum (L_{min}) and maximum (L_{max}) heights of a spinnable forest. These parameters depend on the forest structure and in general are different for different forests. To obtain minimum height L_{min}, we consider a situation when the next bundle is pulled from its very end. One can introduce interconnection density, σ_I, which is the number of interconnections per unit height of the forest. The interconnection density depends only on the forest structure. Then using eq 2, we obtain

$$L_{min} = \frac{f}{f_1} \cdot \frac{1}{\sigma_I} \quad (4)$$

The maximum height, L_{max}, is found by assuming that the next bundle is pulled exactly from the middle. The force required to pull the bundle from the middle is twice higher than the force required to pull it from the end since we should bend two parts of the bundle. Using the higher limit of interconnection density (right part of eq 2) we obtain $L_{max} = 4L_{min}$. In our typical synthesis procedure we obtain the spinnable forest when its height is from 100 to 800 μm. We believe that an experimentally achieved higher upper limit on forest height arises from a 3-D structure of the forest, while in our model we considered a 2-D case. Taking into account the adjacent planes, the termination might not happen when the number of interconnections reaches twice the minimum value (right part of eq 2) but at some higher value. The insights on 3-D structure are provided in the Supporting Information (see Figure S3) and will be the subject of further publications. Also, the forest can be made spinnable at both lower and higher heights as well; however the synthesis conditions have to be adjusted accordingly.

DISCUSSION AND CONCLUSIONS

Though our model is built on an idealized array of uniform CNT bundles with interconnections between them (Figure 1, left, and Figure S3), some properties of CNT forest close to these ideal situation were reported to be necessary for the solid-state dry-drawing of CNT sheets and yarns.[3−6,14] For example, the CNT forest should be vertically aligned in order to be drawable, and some interconnections were shown to exist.[14] Our idealized model shows the relations between different parameters of CNT forest required for drawability, which can guide experimental research on improvement of the synthesis of CNT forests.

The model can help to predict some of the as-produced CNT sheet physical properties. Since the concentration of interconnections is able to transfer the forces from the first bundle to the adjacent one, it is natural that the final sheet structure keeps this strength along the direction of pulling. Contrarily, since the lateral connections between the bundles cannot be concentrated, the lateral stiffness of the CNT sheet should be much smaller than the longitudinal one, which was experimentally observed.[12]

Our model qualitatively explains why taller drawable CNT forests produce more dense CNT sheets (reported by Liu *et al.*[14]). If the number of interconnections is in between the minimum and maximum, the point where the next bundle will start being pulled out will be before its extremity. The part of this bundle that remains in contact with the first bundle will bend and adjust itself along the pulling-out direction. The CNT sheet will, then, have two different regions: one formed by main individual bundles and the other formed by these pairs of bundles in contact. The second region will contribute to increased density of the CNT sheet as well as to smaller total length. Taller CNT forests, according to this model, produce denser CNT sheets, as observed in ref 14.

In a recent work on drawability conditions for vertically aligned CNT (VACNT) forests of different heights and densities,[21] it was proposed that both wavy and low-density VACNT forests are not able to form yarns from a pulling-out process. They also found a range for minimum and maximum VACNT forest heights that are drawable and that some forests with different densities along forest height are not drawable. Our model can qualitatively give insights on these results based on our eq 4. Different forest density will lead to different values of density of interconnections, σ_I, which in turn influences the drawability according to our model. The irregular growth of CNT forest described in ref 21 when using an additional Co layer as catalyst causes lower forest density and, in terms of our model, causes decreasing of the number of interconnections, thus leading this forest to become nondrawable.

The correspondence of the length of the CNT sheet with the "*x*" length of the CNT forest is simple in the case where we have the minimum number of interconnections. If we have N_x bundles per cm along the x axis, the length of the CNT sheet will be $N_x \times L$ cm, where L is the height of the forest. But this result is not a novelty, since the model in ref 4 also predicts the same result.

It is known that the electrical, optical, and heat transport properties of CNT sheets increase with the length of individual CNTs.[22−24] Our model can guide experimentalists to synthesize taller drawable CNT forests to improve these properties.

A model of the structure of a CNT sheet in terms of our model is being developed and will be the subject of a future publication.

In conclusion, a model of the dry-drawing process of CNT sheet formation was developed. The model explains why the vast majority of CNT forests are not drawable, highlighting the most important features on forests' drawability. A parameter, called the number of interconnections, was introduced to the model, and it was shown that for a forest to be drawable, it can only vary in a very limited range. A new dynamical process called "unzipping" was proposed based on peeling off/sticking of interconnections. It requires the pulled bundle to be bent in order to provide the correct difference of forces in the interconnections. To validate the model, several SEM images of the pulling-out process were presented, the critical force for starting the pulling-out process was measured, and the density of a drawn CNT sheet was analyzed in terms of the model. Among the features of a drawable CNT forest, the vertical alignment of thick bundles and the existence of a network of special interconnections are the most important. We also provided a model relating the minimum and maximum CNT forest heights to forces of peeling off small bundles from big bundles, bending forces, and density of interconnections. Recent studies of the CVD process of CNTs has demonstrated that forest parameters described in our model can be tuned by synthesis conditions[25] and proper catalyst treatment.[26] Another recent paper[27] has clarified conditions for spinnability of CVD forests, which together with the present model will help to create stronger CNT sheets and yarns for advanced applications, such as lightweight superconducting wires and cables and many more.

Future analysis will be in terms of pulling out the CNT sheet at a given angle with respect to the $x-y$ plane. Also, studies on local structure of the interconnections between individual CNTs and main bundles will help to provide more precise values for the forces involved in the process. Our model can guide improvements in electrical and optical properties of sheets, such as the sheet resistance anisotropy and quality of optical polarizers. We hope our work will further stimulate both theoretical and experimental efforts toward the development of stronger CNT sheets and yarns with higher electrical conductivity, higher optical transmission, and better degree of polarization.

METHODS

Transparent carbon nanotube aerogel sheets were drawn from straight sidewalls of a multiwalled nanotube forest that were synthesized by catalytic chemical vapor deposition, using acetylene gas as the carbon source.[3] Deployed nanotube forests had heights between 100 and 800 μm, and the drawn sheets contained less than 1 wt % catalyst. From transmission electron microscopy and scanning electron microscopy, the nanotubes had an outer diameter of ~12 nm and contained ~9 walls. The nanotubes in the sheets were highly bundled, with an average of roughly 100 nanotubes in each bundle. Sheet mechanical properties depend on the degree of alignment of the nanotubes in the sheets. This alignment as well as the sheet's drawability depends upon the structural nature of the precursor nanotube forest according to the proposed model.

Acknowledgment. This work was supported by NSF NIRT grant DMI-0609115, AFOSR grant FA 9550-09-1-0384, Office of Naval Research grant STTR N00014-08-M-0323, a grant from the Brazilian agency CNPq (Conselho Nacional de Desenvolvimento Científico e Tecnológico), Robert A. Welch Foundation Grants AT-0029 and AT-1617, AFRL/Rice grant *via* CONTACT consortium, and a HONDA research grant. We thank M. Zhang for help with SEM images and the SEM-based movie (S1) and also for discussions. The assistance of R. Ovalle in making CNT forests of different heights is also highly appreciated.

Supporting Information Available: Material characterization. Extension of the model to the 3-D case. Calculation of forces involved in the unzipping process. Scanning electron microscope movie showing the drawing of CNT sheets. This material is available free of charge *via* the Internet at http://pubs.acs.org.

REFERENCES AND NOTES

1. Jiang, K.; Li, Q.; Fan, S. Nanotechnology: Spinning Continuous Carbon Nanotube Yarns. *Nature* **2002,** *419*, 801.

2. Zhang, M.; Atkinson, K. R.; Baughman, R. H. Multifunctional Carbon Nanotube Yarns by Downsizing an Ancient Technology. *Science* **2004,** *306*, 1358–1361.
3. Zhang, M.; Fang, S.; Zakhidov, A. A.; Lee, S. B.; Aliev, A. E.; Williams, C. D.; Atkinson, K. R.; Baughman, R. H. Strong, Transparent, Multifunctional, Carbon Nanotube Sheets. *Science* **2005,** *309*, 1215–1219.
4. Zhang, X.; Jiang, K.; Feng, C.; Liu, P.; Zhang, L.; Kong, J.; Zhang, T.; Li, Q.; Fan, S. Spinning and Processing Continuous Yarns from 4-Inch Wafer Scale Super-Aligned Carbon Nanotube Arrays. *Adv. Mater.* **2006,** *18*, 1505–1510.
5. Li, Q.; Zhang, X.; De Paula, R. F.; Zheng, L.; Zhao, Y.; Stan, L.; Holesinger, T. G.; Arendt, P. N.; Peterson, D. E.; Zhu, Y. T. Sustained Growth of Ultralong Carbon Nanotube Arrays for Fiber Spinning. *Adv. Mater.* **2006,** *18*, 3160–3163.
6. Zhang, X.; Li, Q.; Tu, Y.; Li, Y.; Coulter, J. Y.; Zheng, L.; Zhao, Y.; Jia, Q.; Peterson, D. E.; Zhi, Y. Strong Carbon-Nanotube Fibers Spun from Long Carbon-Nanotube Arrays. *Small* **2007,** *3*, 244–248.
7. Xiao, L.; Liu, P.; Liu, L.; Jiang, K.; Feng, X.; Wei, Y.; Qian, L.; Fan, S.; Zhang, T. Barium-Functionalized Multiwalled Carbon Nanotube Yarns as Low-Work-Function Thermionic Cathodes. *Appl. Phys. Lett.* **2008,** *92*, 153108.
8. Zhang, S.; Zhu, L.; Minus, M. L.; Chae, H. G.; Jagannathan, S.; Wong, C.-P.; Kowalik, J.; Roberson, L. B.; Kumar, S. Solid-State Spun Fibers and Yarns from 1-mm Long Carbon Nanotube Forests Synthesized by Water-Assisted Chemical Vapor Deposition. *J. Mater. Sci.* **2008,** *43*, 4356–4362.
9. Nakayama, Y. Synthesis, Nanoprocessing, and Yarn Application of Carbon Nanotubes. *Jpn. J. Appl. Phys.* **2008,** *47*, 8149–8156.
10. Tran, C. D.; Humphries, W.; Smith, S. M.; Huynh, C.; Lucas, S. Improving the Tensile Strength of Carbon Nanotube Spun Yarns Using a Modified Spinning Process. *Carbon* **2009,** *47*, 2662–2670.
11. Ray, S.; Nath, S. K.; Kumar, A.; Agarwala, R. C.; Agarwala, V.; Chaudhari, G. P.; Daniel, B. S. S. Study on Carbon Nano-Tube Spun Thread as Piezoresistive Sensor Element. *Adv. Mater. Res.* **2009,** *67*, 155–160.
12. Aliev, A. E.; Oh, J.; Kozlov, M. E.; Kuznetsov, A. A.; Fang, S.; Fonseca, A. F.; Ovalle, R.; Lima, M. D.; Haque, M. H.; Gartstein, Y. N.; *et al*. Giant-Stroke, Superelastic Carbon Nanotube Aerogel Muscles. *Science* **2009,** *323*, 1575–1578.
13. Hall, L. J.; Coluci, V. R.; Galvão, D. S.; Kozlov, M. E.; Zhang, M.; Dantas, S. O.; Baughman, R. H. Sign Change of Poisson's Ratio for Carbon Nanotube Sheets. *Science* **2008,** *320*, 504–507.
14. Liu, K.; Sun, Y.; Chen, L.; Feng, C.; Feng, X.; Jiang, K.; Zhao, Y.; Fan, S. Controlled Growth of Super-Aligned Carbon Nanotube Arrays for Spinning Continuous Unidirectional Sheets with Tunable Physical Properties. *Nano Lett.* **2008,** *8*, 700–705.
15. Kendall, K. Thin-Film Peeling-the Elastic Term. *J. Phys. D: Appl. Phys.* **1975,** *8*, 1449.
16. Coffin, D. W.; Carlsson, L. A.; Pipes, R. B. On the Separation of Carbon Nanotubes. *Compos. Sci. Technol.* **2006,** *66*, 1132–1140.
17. Girifalco, L. A.; Hodak, M.; Lee, R. S. Carbon Nanotubes, Buckyballs, Ropes, and a Universal Graphitic Potential. *Phys. Rev. B* **2000,** *62*, 13104–13110.
18. Strus, M. C.; Zalamea, L.; Raman, A.; Pipes, R. B.; Nguyen, C. V.; Stach, E. A. Peeling Force Spectroscopy: Exposing the Adhesive Nanomechanics of One-Dimensional Nanostructures. *Nano Lett.* **2008,** *8*, 544–550.
19. Yakobson, B. I.; Couchman, L. S. Persistence Length and Nanomechanics of Random Bundles of Nanotubes. *J. Nanopart. Res.* **2006,** *8*, 105–110.
20. DiBiasio, C. M.; Cullinan, M. A.; Culpepper, M. L. Difference between Bending and Stretching Moduli of Single-Walled Carbon Nanotubes that are Modeled as an Elastic Tube. *Appl. Phys. Lett.* **2007,** *90*, 203116.
21. Lee, I. H.; Han, G. H.; Chae, S. J.; Bae, J. J.; Kim, E. S.; Kim, S. M.; Kim, T. H.; Jeong, H.-K.; Lee, Y. H. Criteria for Producing Yarns from Vertically Aligned Carbon Nanotubes. *NANO* **2010,** *5*, 31.
22. Aliev, A. E.; Guthy, C.; Zhang, M.; Fang, S.; Zakhidov, A. A.; Fisher, J. E.; Baughman, R. H. Thermal Transport in MWCNT Sheets and Yarns. *Carbon* **2007,** *45*, 2880–2888.
23. Aliev, A. E.; Fridman, A. A.; Khabibullaev, P. K. Electrical Conductivity of Paper Based on Single-Wall and Multiwall Nanotubes. *J. Commun. Technol. Electron.* **2005,** *50*, 1074–1081.
24. Aliev, A. E.; Kuznetsov, A. A. The Origin of Polarized Blackbody Radiation from Resistively Heated Multiwalled Carbon Nanotubes. *Phys. Lett. A* **2008,** *372*, 4938–4942.
25. Bedewy, M.; Meshot, E. R.; Guo, H.; Verploegen, E. A.; Lu, W.; Hart, A. J. Collective Mechanism for the Evolution and Self-Termination of Vertically Aligned Carbon Nanotube Growth. *J. Phys. Chem.* **2009,** *113*, 20576–20582.
26. Meshot, E. R.; Plata, D. L.; Tawfick, S.; Zhang, Y.; Verploegen, E. A.; Hart, A. J. Engineering Vertically Aligned Carbon Nanotube Growth by Decoupled Thermal Treatment of Precursor and Catalyst. *ACS Nano* **2009,** *3*, 2477–2486.
27. Huynh, C. P.; Hawkins, S. C. Understanding the Synthesis of Directly Spinnable Carbon Nanotube Forests. *Carbon* **2010,** *48*, 1105.